

SAHA Enhances Differentiation of CD34+CD45+ Hematopoietic Stem and Progenitor Cells from Pluripotent Stem Cells Concomitant with an Increase in Hemogenic Endothelium

Seon-Hui Shim¹, Dejene Tufa¹, Renee Woods¹, Trahan D. George¹, Tyler Shank¹, Ashley Yingst¹, Jessica Lake¹, Laura Cobb¹, Dallas Jones¹, Kenneth Jones², Michael R. Verneris^{1,*}

¹University of Colorado and Children's Hospital of Colorado, Department of Children's Cancer and Blood Disorders, Aurora, CO, USA

²Department of Cell Biology, University of Oklahoma School of Medicine, Oklahoma City, OK, USA

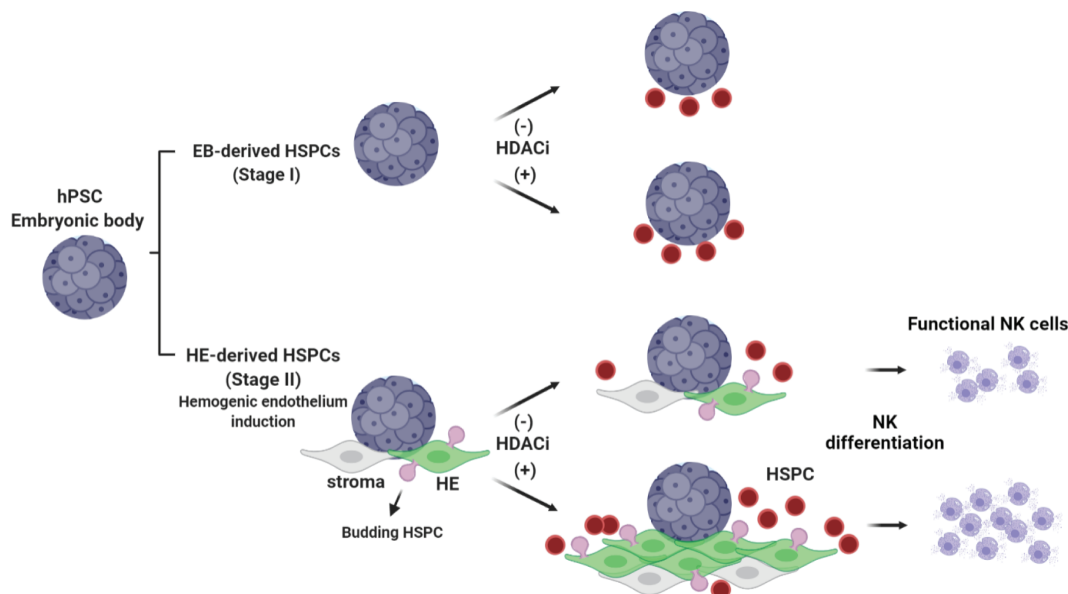
*Corresponding author: Michael R. Verneris, MD, Pediatric Bone Marrow Transplantation and Cellular Therapy, University of Colorado Anschutz Medical Campus Research Complex 1, North Tower 12800 E. 19th Avenue, Mail Stop 8302 Room P18-4108, Aurora, CO 80045, USA. Tel: +1 303 724-4634; Email: michael.verneris@cuanschutz.edu

Abstract

Epigenetic modification is an important process during hematopoietic cell differentiation. Histone deacetylase (HDAC) inhibitors have previously been shown to enhance expansion of umbilical cord blood-derived hematopoietic stem cells (HSCs). However, the effect of HDAC inhibitors on pluripotent stem cells (PSCs) in this context is less understood. For years, investigators have considered PSC-derived natural killer (NK) and T-cell therapies. These "off-the-shelf" cellular therapies are now entering the clinic. However, the *in vitro* commitment of PSCs to the hematopoietic lineage is inefficient and represents a major bottleneck. We investigated whether HDAC inhibitors (HDACi) influence human PSC differentiation into CD34+CD45+ hematopoietic stem and progenitor cells (HSPCs), focusing on hemogenic endothelium (HE). Pluripotent stem cells cultured in the presence of HDACi showed a 2-5 times increase in HSPCs. Concurrent with this, HDACi-treated PSCs increased expression of 7 transcription factors (HOXA5, HOXA9, HOXA10, RUNX1, ERG, SPI1, and LCOR) recently shown to convert HE to HSPCs. ChIP-qPCR showed that SAHA upregulated acetylated-H3 at the promoter region of the above key genes. SAHA-treated human PSC-derived CD34+CD45+ cells showed primary engraftment in immunodeficient mice, but not serial transplantation. We further demonstrate that SAHA-derived HSPCs could differentiate into functional NK cells *in vitro*. The addition of SAHA is an easy and effective approach to overcoming the bottleneck in the transition from PSC to HSPCs for "off-the-shelf" cellular immunotherapy.

Key words: HDAC inhibitor; CD34+CD45+; stem cells; hemogenic endothelium; HSPC; hematopoietic progenitors.

Graphical Abstract



Received: 17 August 2021; Accepted: 27 January 2022.

© The Author(s) 2022. Published by Oxford University Press.

This is an Open Access article distributed under the terms of the Creative Commons Attribution-NonCommercial License (<https://creativecommons.org/licenses/by-nc/4.0/>), which permits non-commercial re-use, distribution, and reproduction in any medium, provided the original work is properly cited. For commercial re-use, please contact journals.permissions@oup.com.

Introduction

Cellular immunotherapy has been transformative for some malignancies. For instance, chimeric antigen receptor (CAR) T cells have shown profound activity in patients with refractory leukemia and lymphoma.^{1,2} Likewise, manipulation of NK cells, either with or without CARs, has also shown promise in refractory B cell and myeloid malignancies.^{3,4} However, the production of adoptive cellular immune therapy is burdensome for both the patient and the medical provider. For commercial sources of CAR T-cell therapy, patient lymphocytes must be collected by apheresis, cryopreserved and then transferred to the good manufacturing facility where the cells are produced. Then, once the cells meet quality control measures, they are ultimately shipped back to the center and infused into the patient. This individualized process is laborious, slow, and costly. The use of pluripotent stem cells (PSCs) as a source of “off-the-shelf” cellular therapies has been considered for both NK-cell- and T-cell-based therapies.^{5,6} The benefits of “off-the-shelf” cellular therapy are numerous and include economies of scale and the ability to genetically modify the cells with the goal of enhanced tumor homing, recognition, cytotoxicity, and/or survival. Because PSCs can be serially passaged, such gene edits would need to be performed only once and many patients could be treated with a more standardized cell therapy product. However, the differentiation of PSCs to hematopoietic stem cells (HSCs) and progenitor cells (HSPC) is inefficient and costly. Methods to accelerate the transition of PSCs to HSPCs would be significantly impactful.

HDAC inhibitors have been tested for their ability to expand umbilical cord blood (UCB)-derived-HSCs.⁷⁻⁹ HDAC inhibitors (TSA and Chlamydocin) enhance murine HSC expansion and engraftment.¹⁰ Recently, nicotinamide, an inhibitor of the NAD-dependent class III HDAC, was tested on UCB-derived CD34+ HSCs and led to hematopoietic progenitor cell expansion, enhanced engraftment in murine models, as well as encouraging results in early human clinical trials.¹¹⁻¹³ Based on these data, we hypothesized that HDAC inhibitors might also act prior to HSC commitment and influence the differentiation of PSCs into the hematopoietic lineage (ie, into CD34+CD45+ cells). To test this, we compared the impact of HDAC inhibitors in 2 differentiation systems. The first is the stage I system which results in CD34+CD45+ cells derived directly from embryonic bodies (EBs; Fig. 1A). The second method is the stage II system which starts with EBs that are then transferred to flat bottom plates and give rise to both hemogenic endothelium (HE) and CD34+CD45+ cells (Fig. 1B).

HE produces HSCs through a process known as endothelial-to-hematopoietic transition.¹⁴ PSC-derived HSCs can transit through a HE stage which is transient and infrequent.^{15,16} By differentiating induced pluripotent stem (iPSC) cells into HSCs and using single-cell RNA sequencing, Carolina et al molecularly defined HE.¹⁷ Sugimura et al showed that induced expression of 7 transcription factors (HOXA5, HOXA9, HOXA10, RUNX1, SPI1, ERG, and LCOR) was sufficient to convert HE to HSCs and that these cells can durably engraft in immune deficient mice.¹⁸

We investigated whether HDAC inhibitors might preferentially facilitate the development of PSC-derived HSPCs (CD34+CD45+ cells). Through these studies, we show that HDAC inhibitors increased the generation of HE and their development into CD34+CD45+ cells. By adding HDAC

inhibitors to differentiation cultures, we noted the expression of various transcription factors previously associated with an “engraftable” PSC-derived CD34+CD45+ cells described by Sugimura¹⁸ and confirmed their expression was HDAC-driven via the presence of acetylated-H3 bound to the promoter of these genes. CD34+CD45+ cells differentiated in the presence of the HDAC inhibitor, SAHA, and resulted in enhanced engraftment following primary bone marrow transplantation in immune deficient mice. These data show that HDAC inhibitors increase the differentiation of CD34+CD45+ HSPCs from PSCs, via HE. As well, SAHA generated PSC-derived CD34+CD45+ cells could be differentiated into the NK lineage in vitro, generating significantly higher numbers of these effector cells. Collectively, these studies suggest HDAC inhibitors can increase the commitment of PSCs to CD34+CD45+ HSPCs, representing an easy and rapidly translatable approach to the generation of “off-the-shelf” cellular therapy.

Materials and Methods

Differentiation of hESCs into HPSCs and NK Cells

Single-cell adapted hESCs (H9) and human iPSC cells were maintained on irradiated mouse embryonic fibroblasts in embryonic stem cell growth media, as previously described.⁶ hESCs were differentiated using spin embryoid bodies (EBs). In brief, hESCs and iPSCs were plated at 3000 cells and 8000 cells, respectively, per 100 μ L in a round-bottom 96-well plate using serum-free bovine serum albumin polyvinyl alcohol essential lipid (BPEL) media supplemented with 20 ng/mL bone morphogenetic protein 4 (BMP4, R&D Systems, Minneapolis, MN), 40 ng/mL stem cell factor (SCF, STEMCELL Technologies, Vancouver, BC, Canada), and 20 ng/mL vascular endothelial growth factor (VEGF, STEMCELL Technologies). Cells were centrifuged to form EBs with 1250 rcf (defined as day 0) and were incubated for 7 days (defined as day 7) to promote mesoderm induction. To produce HSPC differentiation directly from EBs, we used the stage I differentiation method shown in Fig. 1A. EBs were cultured in U-bottom plates during the entire culture period and at day 7, the media was changed to BPEL media (without polyvinyl alcohol), supplemented with 40 ng/mL SCF, 40 ng/mL VEGF, 30 mg/mL thrombopoietin (all from STEMCELL Technologies), 30 ng/mL IL-3, and 30 ng/mL IL-6 (both R&D Systems, Minneapolis, MN). After changing the media, EBs were cultured for an additional 7-10 days (defined as day 7 + 7/10). To differentiate early endothelial and HSCs (Fig. 1B), day 7 EBs were transferred to pregelatinized 24-well plates with BPEL media (without polyvinyl alcohol) supplemented with the same cytokines as stage I. EBs were treated at day 7 + 0 with either dimethyl sulfoxide (DMSO), 200 nM SAHA (suberanilohydroxamic acid, Vorinostat) (Sigma-Aldrich, St. Louis, MO), or 50 nM TSA (Trichostatin A) (Sigma-Aldrich, St. Louis, MO). Media was exchanged every 3 days with or without HDAC inhibitors and cytokine supplementation. For the stage I, day 7 EBs had the changed media every 3 days with the same cytokines as stage II. At indicated times, non-adherent cell fractions were collected for further analysis. For the NK differentiation, EBs were collected and analyzed by flow cytometry to assess HSPC potential (CD34+CD45+) and the HSPCs were transferred onto 24-well plates coated with irradiated OP9-DL4. EBs and OP9-DL4 were cocultured in NK differentiation media (B0 media) supplemented with SCF,

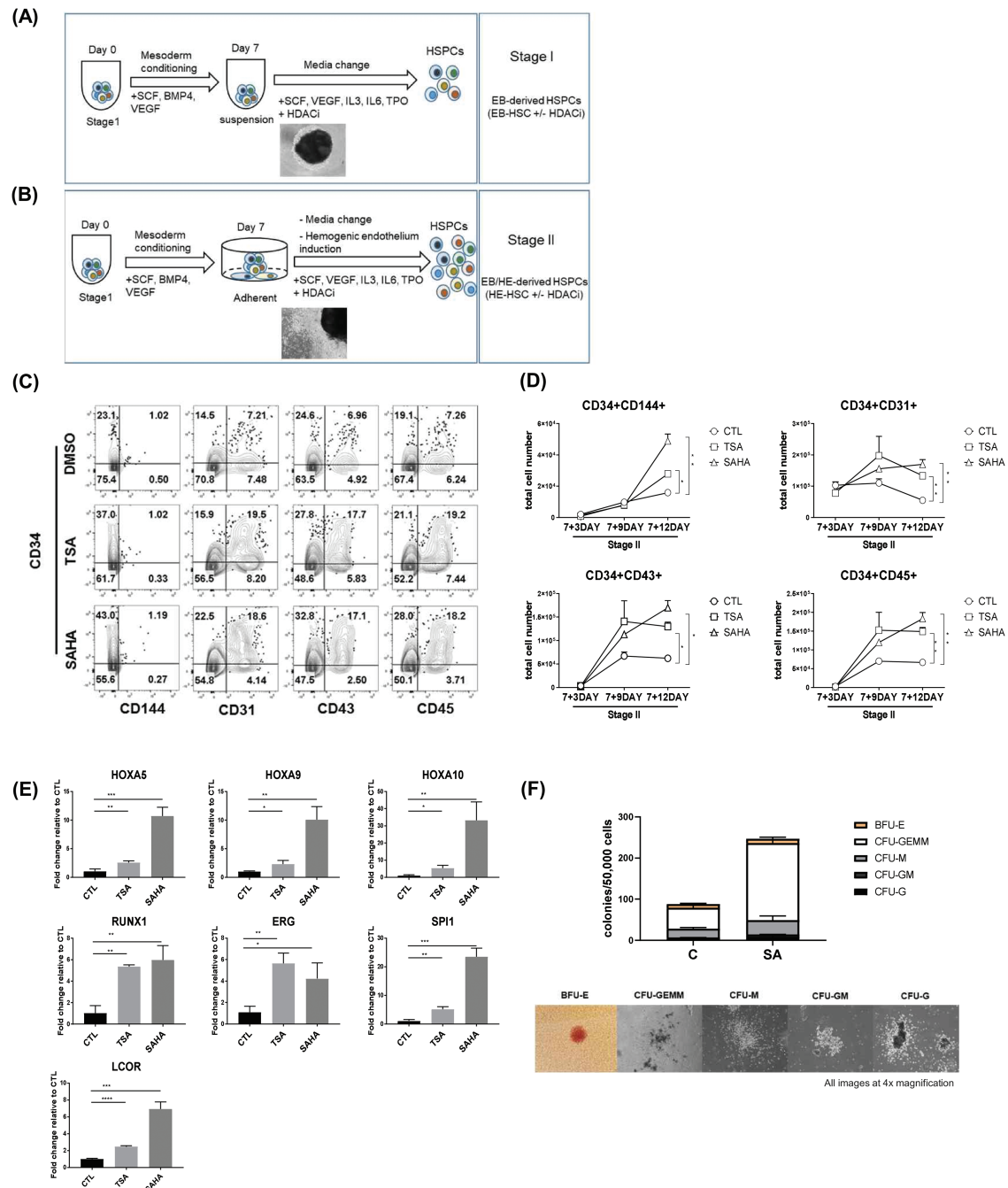


Figure 1. HDAC inhibitor increased HSPCs from hESCs by stage II system. **(A)** Stage I system. A schematic of hESC differentiation into HSPCs using the stage I, spin EB method. At day 0, ES cells are plated in a round bottom 96-well plate and spun to make embryonic body. At day 7, media was changed with BPEL media (without PVA) in the same round bottom plates with defined cytokines and either 200 nM SAHA, 50 nM TSA, or DMSO vehicle every 3 days. The EB image was captured at day 7 + 10. **(B)** Stage II system, from days 0 to 7, the spin EB method used was the same as the stage I system. At day 7, EBs are transferred into hematoendothelial culture media (stage II media) to promote endothelial and hematopoietic cell differentiation. Also at day 7, cells are treated with either 200 nM SAHA, 50 nM TSA, or DMSO vehicle with media changing in both stages I and II. **(C)** Representative FACS plots of hESC differentiation from the stage II system with 50 nM TSA, 200 nM SAHA, and DMSO. All differentiated cell fractions were harvested at day 7 + 10. Cells were assessed for CD34+CD144+, CD34+CD31+, CD34+CD43+, and CD34+CD45+. **(D)** Absolute cell numbers of CD34+CD144+, CD34+CD31+, CD34+CD43+, and CD34+CD45+ at days 7 + 3, 7 + 9, and 7 + 12; $n = 3-5$, error bars represent standard error of the mean (SD), 2-way ANOVA and significance is shown $*P < .05$; $**P < .01$. **(E)** Both adherent and non-adherent cell fractions differentiated using the stage II system from hESCs are harvested at day 7 + 3 and probed for gene expression of the 7 genes by qRT-PCR. For each gene, cycle threshold (Ct) values were normalized to β -actin at each time point and the data are presented as relative fold change to DMSO-treated controls; $n = 3$, error bars represent mean \pm SD; $*P < .05$; $**P < .01$; $***P < .001$, $****P < .0001$ using the unpaired t test. **(F)** Colony forming unit assay of stage II differentiated cells. Cells were harvested at day 7 + 6 and seeded at 50 000 cells per dish in a standard methylcellulose-based media. Colonies were counted for each treatment group following 14 days of culture and scored for the following morphological subsets: burst forming unit-erythroid (BFU-E); CFU-granulocyte (CFU-G); CFU-macrophage (CFU-M); CFU-granulocyte, macrophage (CFU-GM); CFU-granulocyte, erythroid, macrophage, megakaryocyte (CFU-GEMM); $n = 4$, error bars represent SD of the total number of colonies per 50 000 cells seeded. $P = .0001$ 1-way analysis of variance (ANOVA).

IL-15, IL-7, Flt3-L, and IL-3 for 1 week.¹⁹ Every week, a one-half media change with B0 media supplemented with SCF, IL-15, IL-7, and Flt3-L. Cells were differentiated for 3 weeks.

Hematopoietic Colony-Forming Unit Assay

Single suspension cells from stage II differentiation at day 7 + 6 were collected and resuspended in IMDM. Fifty thousand cells were seeded in 3 mL of H4436 Methocult (STEMCELL Technologies) and plated directly in 35-mm culture dishes (Greiner, Monroe, NC). After culture for 14 days, the colonies were counted and scored using standard criteria.

Flow Cytometry

The following antibodies were used (all anti-human): CD144-Percp-Cy5.5 (Biolegend), CD90-APC (Biolegend), CD31-PE-Cy7 (BD Biosciences), CD34-APC (BD Biosciences), CD34-PE (BD Bioscience), CD43-BV421 (BD Biosciences), CD45-APC-Cy7 (Biolegend), and CD45-BV605 (BD Bioscience). Samples were analyzed on Celesta or LSRII (BD Biosciences). Data from flow cytometry were analyzed using FlowJo software (TreeStar, Ashland, OR).

RNA-Sequencing (RNA-seq)

CD34+CD45+ cells from stages I and II differentiation at day 7 + 3 were first sorted from each stage using FACS, then RNA was purified with the RNeasy Micro kit (Qiagen). RNA libraries were sequenced as 151 bp paired-end reads on the Illumina NovaSeq 6000 platform at the University of Colorado's Genomics Core Facility. Read quality was assessed using FastQC v0.11.7 and multiQC v1.7.dev0 both before and after trimming, which was performed using BBDuk v38.70. Reads were quasi-mapped to the GRCh38.p13 reference transcriptome (GENCODE, gencode. v32. transcripts. fa) using Salmon v0.14.1 in order to obtain transcript-level counts.

Differential Expression and Gene Set Enrichment Analyses

Within an R v3.6.1 environment, Tximport v1.12.3 was used to summate transcript counts at the gene level using the information contained in the aforementioned GENCODE FASTA file. DESeq2 v1.24.0 was then used to perform differential expression analysis on genes with at least 1 count across all samples. Log₂ (fold change) values were shrunk using the apeglm algorithm within DESeq2. For enrichment analysis, all samples were compared to the stage I C group and genes with less than 10 counts across all samples were removed; for each comparison, genes were ranked by $-\log_{10}$ (*P*-value). For genes that had their *P*-value rounded to 0, the $-\log_{10}$ (*P*-value) was set to the highest unrounded $-\log_{10}$ (*P*-value) and the corresponding absolute apeglm shrunken log₂ (fold change) was added. GAGE v2.34.0 was used to determine KEGG pathway enrichment in the pre-ranked gene lists. A *q*-value of 0.25 was used as the threshold to identify statistically significant pathways.

In Vivo Analysis

NSG mice (The Jackson Laboratory) were bred and housed at the University of Colorado Denver, Anschutz Medical Campus animal care facility. All procedures were approved by the Institutional Animal Care and Use Committee at the University of Colorado Denver, Anschutz Medical Campus.

Six- to 10-week-old mice were irradiated (220 rad) and then 12 hours later received transplantation intrafemoral injection. Before transplantation, mice were anesthetized with isoflurane. A 27-gauge needle was inserted into the femur and 1×10^6 hESCs-derived HSPCs were transplanted in a 25- μ L volume. Uniprim (ENVIGO) was administered as food to prevent infections after irradiation. Mice were sacrificed 10-12 weeks post-injection to collect bone marrow (BM) mononuclear cells for analysis. Secondary transplantation used the same methods described above.

Quantitative PCR

RNA extraction was performed using an RNeasy Mini kit (Qiagen). Reverse transcription was performed using iScript cDNA synthesis kit (Bio-Rad). Quantitative PCR was performed in triplicate with SYBR Green (Quanta bio). Transcript abundance was calculated using the standard curve method. Primers used for this study were as follows: SPI1 F-GCGACCATTACTGG-GACTTCC, R-GGGTATCGAGGACGTGCAT, HOXA10 F-CTCGCCCATAGACCTGTGG, R-GT TCTGCGCG AAAGAGCAC, HOXA9 F-CTGTCCCACGCTTGACACTC, R-CTCCGCCGCTCTC ATTCTC, HOXA5 F-TACGGCTAC AATGGCATGGATR-CCGCTGGAGTTGATTAGGG, LCOR F-ATGCAGCGAATGATCCAACAA R-CCAGAGGTGA GTATTGGTCAG, RUNX1 F-GAAGTCTGAACCCAGCATA GTGGTCAGCAG R-GTGGACGTCTCTAGAATTCATTCC AAG, and ERG F-CGTG CCAGCAGATCCTACG R-GGTGAGCCTCTGGAAGTCG.

Chip qPCR

At day 7 + 6, after differentiating HE-derived HSPCs, all fractions of cells were collected, and chromatin immunoprecipitation (CHIP) was performed with SimpleChip enzymatic chromatin IP Kit (CellSignaling Technology). All procedures were followed the manufacture's protocol. Primers used for the CHIP qPCR were as follows: HOXA5 F-GGCTCCGAAAGACTCAAGTAA R-AGAGT CCTGGCTTCCAGA, LCOR F-AGATGGCGA GGGTGTGTA R-CCTACACAGTGAATG AGCTTGT, HOXA9 F-GGGGAGACGGGAGAGTACAG R-CGTCCAG CAGAACAATAACG, SPI1 F-CCCTCCCTT GACATTGC R-AGCGCAAGAGATTTATGCAAAC, ERG F-AGGCACCAGCAAC TTCA R-GCATTGAATTCT ATATTTGCTCAGT, and RUNX1 F-ACGCACACG CAACTTCA R-TTTGA ATTAAGTGGCTTCTTGGC.

In Vitro Tumor Growth Assay

To test of tumor growth after adding NK cells derived from the stage II, CD34+CD45+ cells were differentiated for 4 weeks on irradiated OP9-DL4. Differentiated NK cells were stimulated with 10 ng/mL IL-12 and 10 ng/mL IL-18 for overnight. NK cells were then cocultured with the pre-seeded mCherry expressing RH30 cells at 1:1 ET ratio in 96-well plate using B0 media. The plates were scanned every 2 for 24 hours by using InCuCyte. The surviving tumor cells were detected with mCherry expression.

Statistics

Statistical analysis was performed using GraphPad Prism software (GraphPad, San Diego, CA). Paired *t*-test and un-paired *t*-test were used when statistical analysis was required between 2 experimental groups. One-way analysis of variance

(ANOVA) was used when comparisons between multiple groups were required. Two-way ANOVA with repeated measures was used to analyze data with 2 variables such as time and treatment. Data are presented as the \pm SEM. *P*-values of $<.05$ (*), $<.01$ (**), $<.001$ (***), or $<.0001$ (****) were considered statistically significant.

Results

HDACi Increased HSPCs from hESCs

We tested the effect of HDAC inhibitors using 2 different protocols for HSPC differentiation, called stages I and II.⁶ As shown in Fig. 1A, stage I involves direct differentiation of HSPCs from EBs, while the stage II method employs an additional step where the EB is transferred to a flat well plate to generate HE (and other adherent cells) in addition to HSPCs (Fig. 1B). In the presence of 2 different HDAC inhibitors, TSA and SAHA, we used FACS to assess the percentage of HSPCs (CD34+CD144+, CD34+CD31+, CD34+CD43+ and CD34+CD45+) at the end of the culture period (7 + 12 days). Each of these populations were significantly increased by 2- to 5-fold with the addition of the HDAC inhibitors in stage II differentiation system (Fig. 1C and D). Previously, Sugimura et al identified 7 transcription factors that, when over expressed by lentiviral transduction were sufficient to convert HE into engraftable HSCs.¹⁸ As shown in Fig. 1E, both HDAC inhibitors increased the mRNA expression of all 7 genes (HOXA5, HOXA9, HOXA10, RUNX1, ERG, SPI1, and LCOR), but SAHA increased these significantly more than TSA. To test whether HDACi increase the CD34+CD45+ HSPCs from iPSCs, 2 iPSC lines were differentiated with the stage II system. Similar to ESC-derived cells, SAHA increased the percentage and absolute numbers of iPSC-derived CD34+CD45+ cells compared with vehicle control (Supplementary Fig. 1A). In the case of the iPSC-1 line, all of the above 7 genes were upregulated in the presence of SAHA. However, in iPSC-2 line, 6 genes (HOXA5, HOXA9, HOXA10, RUNX1, ERG, and LCOR) were upregulated, but SP1 was not (Supplementary Fig. 1B). Next, we tested the effect of SAHA on colony formation using a methylcellulose-based colony-forming unit (CFU) assay. As shown in Fig. 1F, the hematopoietic progenitor cells from SAHA cultures increased the total number of colonies compared with DMSO controls and this was mainly driven by the increase in CFU-GEMM. Taken together, the addition of either SAHA or TSA increased hESC/iPSC differentiation into HSPCs. Given that SAHA more significantly expanded HSPCs, we chose to focus on this HDACi in subsequent experiments.

HDACi Influenced the Differentiation of HE Cells

The stage II culture system gives rise to multiple cell populations, including adherent, fibroblast-appearing cells some of which are HE.⁶ To characterize the proportion that were HE, we washed off the EB and removed all suspension cells and then stained the adherent cells with antibodies against CD34, CD90, CD43, CD31, and CD45 for FACS. Carolina et al defined HE to be marked by a CD34+CD90+CD45-CD43- phenotype.¹⁷ In addition, the HE cells (CD34+CD90+CD45-CD43-) also expressed CD31+ in our system (Supplementary Fig. S2). CD31 expression is also found from yolk sac derived-lymphohematopoietic endothelial cells which generated lymphohematopoietic cells.²⁰ As shown in Fig. 2A, in the DMSO-treated controls, ~20%-50% of the adherent

cells were HE defined as being CD34+CD90+CD45-.¹⁷ Interestingly, in the presence of SAHA, higher proportions of CD34+CD90+CD45- cells were present (Fig. 2A), perhaps suggesting that SAHA increased the differentiation of EB-derived HE. We next assessed whether these cells could produce HSPCs, which would additionally be supportive of these being HE. After washing off the EBs and other suspension cells and culturing the adherent cells, we found that SAHA containing cultures had an increased proportion of CD34+CD43+ and CD34+CD45+ cells (Fig. 2B). Furthermore, we also observed the budding of suspension cells from the adherent ones (Supplementary Fig. S3). Collectively, these data show an increase in HE-derived HSPCs in the stage II culture system under the influence of SAHA.

Next, we tested whether the addition of SAHA to the stage I system could also increase CD34+CD45+ cells instead of stage II. In case of the stage I system, no differences were shown between control and SAHA condition to produce the CD34+CD45+ HSPCs (Fig. 2C). Comparing CD34+CD90+, CD34+CD43+ and CD34+CD45+ from the stages I and II culture systems, we found that SAHA enhanced each cell population in the stage II culture system, but that it only significantly increased CD34+CD43+ cells in the stage I system, while CD34+CD90+ and CD34+CD45+ cell populations were not significantly changed from controls (Fig. 2D and E). Additionally, we tested whether HDACi also affected the differentiation of UCB-derived HSPCs (CD34+ cells). As previously described, an increase in the percentage of CD34+CD45+ cells was observed with SAHA (Supplementary Fig. S4).⁷⁻⁹ However, the change in the 7 gene signature in SAHA-treated CD34+ cells from UCB was minimal and non-consistent across donors (Supplementary Fig. S5). Similarly, nicotinamide has significant impact on UCB-derived CD34+ cells with respect to expansion and homing.¹¹ We tested whether this class III HDACi might have a similar influence on ES-derived HSPCs, however there was no impact on the generation of CD34+ cells (not shown). Taken together, these data show that SAHA increases the proportion of HE cells and HSPCs in the stage II, but not the stage I culture system. These data also show that SAHA drives the generation of HE-derived HSPCs (present in the stage II developmental system), but not in already developed HSPCs (from UCB).

Gene Analysis Between Stage I-Derived and Stage II-Derived HSPCs

To understand the impact of SAHA on the gene expression from stages I- and stage II-derived HSPCs, we FACS sorted CD34+CD45+ cells at day 7 + 3 from each culture system generated with either DMSO (control) or SAHA and performed RNA sequencing. The fairly large overlap of enriched KEGG pathways ($q \leq 0.25$) shown in Fig. 3A suggests that differences arising from stage II-derived HSPCs and SAHA treatment act on genes within relatively select pathways, as opposed to broadly changing gene expression. Given that the hESCs are in a cytokine-rich environment that promotes HSPC differentiation, it is not surprising that the hematopoietic cell lineage gene set appeared in all comparisons (see Supplementary Table S1 for a list of all significant pathways in each comparison). Based on the enriched KEGG pathway analysis, we investigated individual gene changes, focusing on the hematopoietic cell lineage gene set. Genes were divided into 4 categories: HSC stemness, platelet-related, monocyte related, and adaptive immune (T or B cell) related. In Fig. 3B,

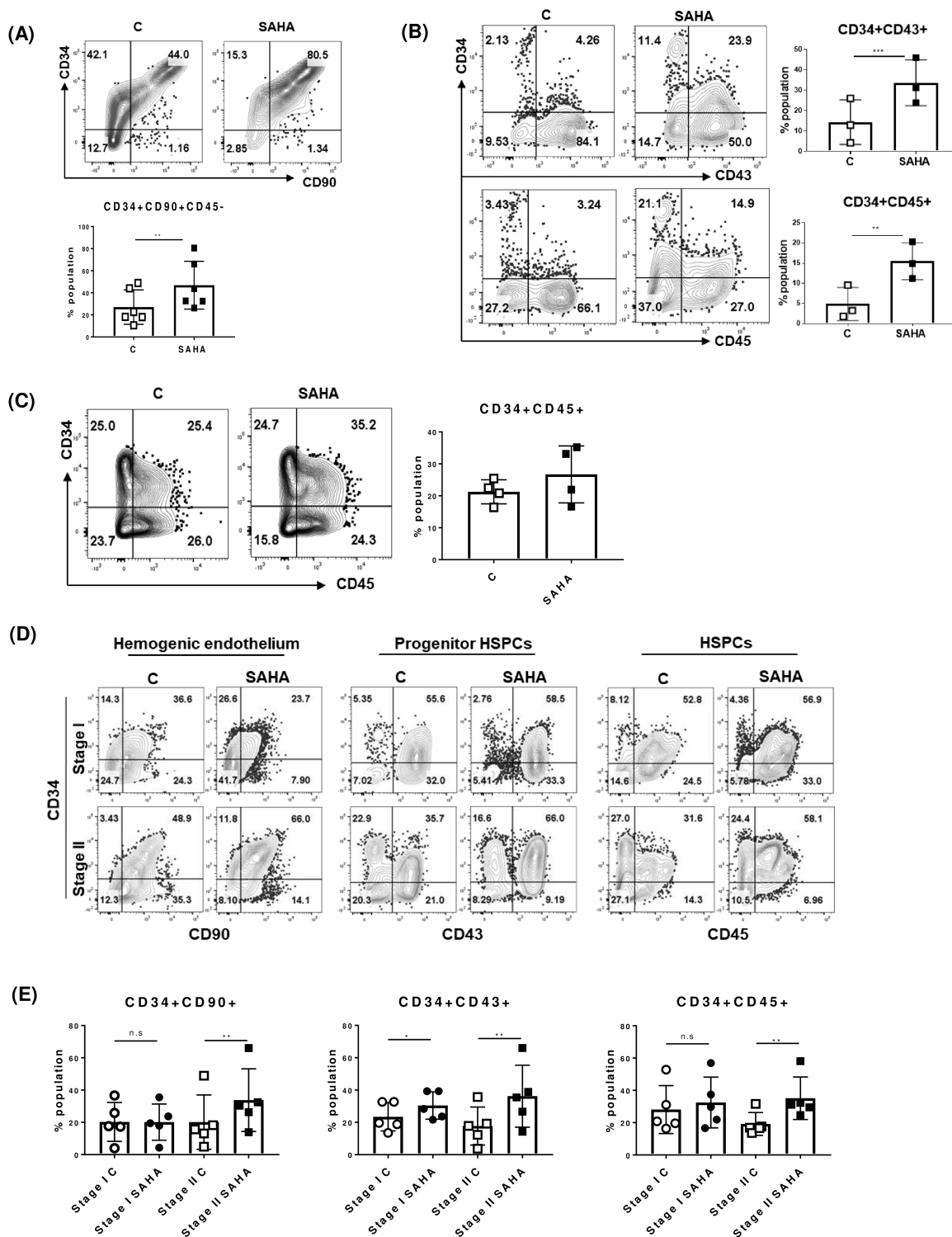


Figure 2. SAHA enhanced the differentiation of HE cells. **(A)** Representative FACS analysis of hemogenic endothelium (HE) cells. After EBs were transferred to flat bottom plates, all EBs and suspension cells were washed at day 7 + 3 of stage II system. Only adherent cells were stained with CD34+CD90+CD45⁻ (HE). The bar graph shows total percentage of CD34+CD90+CD45⁻; *n* = 6, paired *t*-tests and ***P* < .01. **(B)** Representative FACS plots after washing all suspension portion of cells. After transferring EBs at day 7, all cells and EBs were washed at day 7 + 3 and cultured for an additional 9-10 days in either DMSO (control, C) or 200 nM of SAHA. The bar graphs indicate percentage of CD34+CD43⁺ (progenitor of HSPC) and CD34+CD45⁺ (HSPC); *n* = 3, error bars represent SD, ***P* < .01, ****P* < .001, using the paired *t*-test. **(C)** HSPC differentiation by using stage I system. EBs were cultured with stage I system and 200 nM SAHA or DMSO were treated at day 7 + 0 and cells were harvested at day 7 + 6. The bar graph represents that the percentage of CD34+CD45⁺ cells is not significant; *n* = 3, error bars represent mean ± SD. **(D and E)** Comparison of stages I and stage II. Representative FACS plots of hESC differentiation from the stages I and II systems at day 7 + 6. CD34+CD90⁺ (HE), CD34+CD43⁺ (progenitor of HSPCs) and CD34+CD45⁺ (HSPCs); *n* = 5, error bars represent standard error of the mean (SD), paired *t*-test and significance is shown **P* < .05; ***P* < .01.

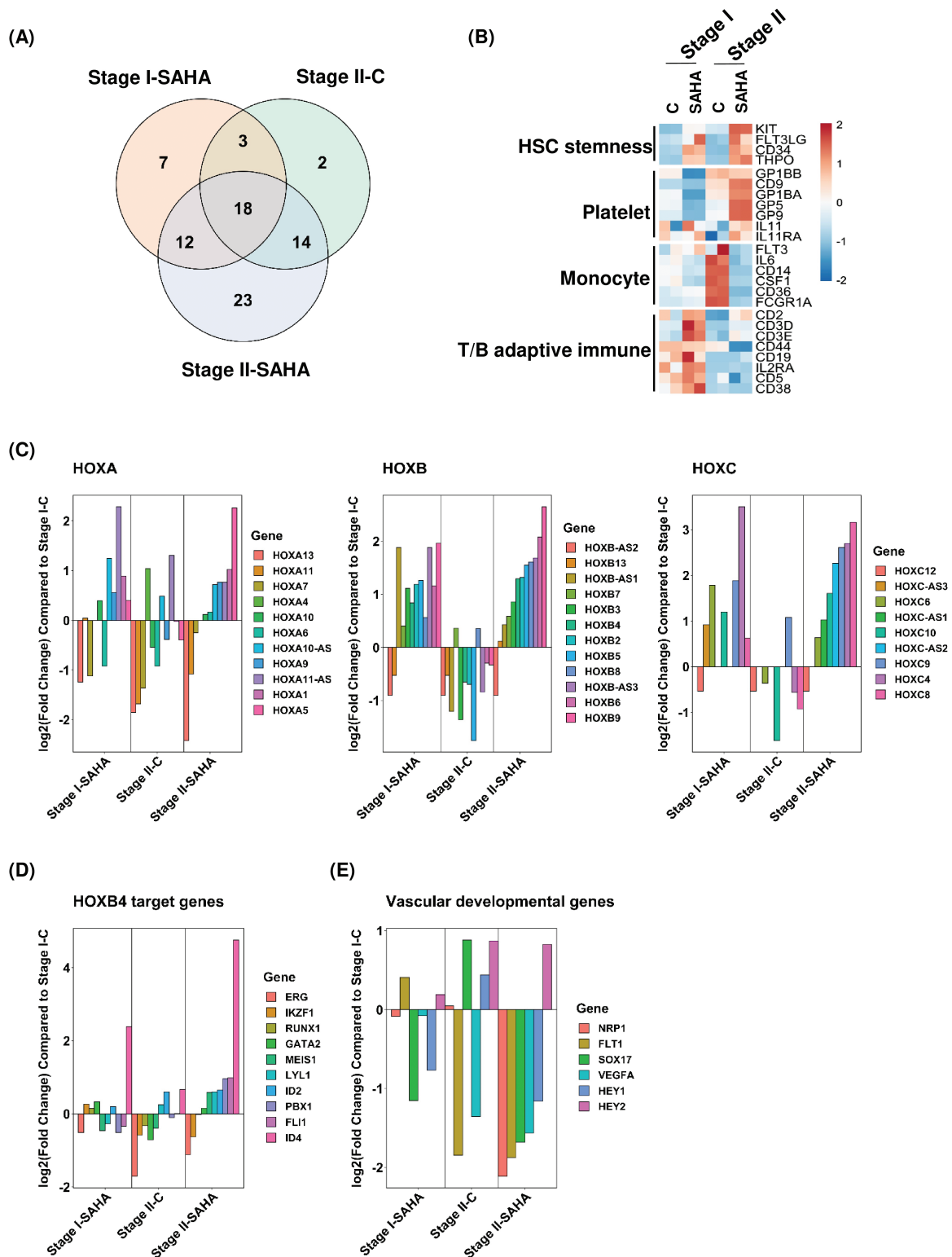


Figure 3. Gene analysis between stage I- and stage II-derived HSPCs. **(A)** Venn diagram showing the overlap of enriched KEGG pathways ($q \leq 0.25$) for each group compared with the stage I-C (DMSO) condition. **(B)** Heat map showing a subset of genes from the hematopoietic cell lineage KEGG pathway grouped by cell type. The color bar represents standardized gene expression. Bar plots showing relative expression for **(C)** HOXA, HOXB, and HOXC cluster genes, as well as **(D)** subsets of HOXB4 downstream targets and **(E)** genes related to vascular development. Log₂ (fold change) values are relative to the stage I-C condition, with genes ordered by stage II-SAHA values.

SAHA-treated stages I- and stage II-derived HSPCs showed an increase in KIT, FLT3, CD34, and TPO, all of which are known to facilitate HSC maintenance. However, the extent of overexpression of these stemness genes was highest in

SAHA-treated stage II cultures. Interestingly, platelet-related genes were also overexpressed in the stage II HSPCs differentiated with SAHA. Stage II HSPCs differentiated without SAHA showed an upregulation of monocyte lineage-related

genes. In stage I cultures, we found increases in the adaptive immunity-related genes, such as CD3 and CD19, which was further augmented by SAHA.

We also focused on the HOX cluster genes since they are critically involved in early hematopoiesis.²¹ Consistent with the above findings, SAHA increased HOX A, B, and C cluster gene expression in both culture systems, but to a larger extent in the stage II-derived HSPCs which overexpressed all the HOXB and HOXC cluster genes (except for HOXC12, Fig. 3C). This suggests SAHA may promote hESC commitment to the hematopoietic lineage, particularly in the stage II-derived HSPCs, through increased HOX cluster gene expression. Fan et al reported that HOXB4 functions as a master regulator of hematopoiesis by regulating multiple hematopoietic transcription factors and chromatin modification enzymes.²² HOXB4 target genes such as ID4, FLI1, PBX1, ID2, LYL1, MEIS1, GATA2, and RUNX1 were also upregulated in the stage II-derived HSPCs with SAHA (Fig. 3D). Moreover, Dou et al described differentially expressed genes between fetal liver hematopoietic progenitor cells (FL-HSPCs) and hESC-derived HSPCs (ES-HSPCs) using microarray analysis.²³ FL-HSPCs, which engrafted efficiently *in vivo*, showed lower expression of vascular development related genes (NRP1, FLT1, SOX17, VEGFA, HEY1, and HEY2) compared with ES-HSPCs. Examining stage II-derived HSPCs cultured in SAHA in a similar manner, showed downregulation of these same genes, except for HEY2. Stage II-derived HSPCs treated with SAHA also showed enhanced cell adhesion and chemokine signaling by KEGG analysis (Supplementary Fig. S6A and B). These latter 2 pathways are potentially involved in homing and engraftment of HSPCs.²⁴⁻²⁶ Additionally, to understand the change of gene expression with multiple approaches, we analyzed the most differentially expressed genes (DEGs) between cells in the various conditions. The top 200 upregulated genes in SAHA expanded CD34+CD45+ cells are shown in Supplementary Fig. S6C. Collectively, these data show that under the influence of SAHA, stage II HSPCs tend to be enriched for genes that enhance HSPC stemness, overexpress HOX cluster genes and downregulate genes associated with vascular development.

Inhibition of HDAC Class II Enhances the Stage II-Derived HSPCs and 7 Gene Overexpression

SAHA is a pan-HDAC inhibitor and it is unclear whether the above findings are mediated by the inhibition of HDAC I, II, III or some combination thereof. To mechanistically dissect the specific class of HDACs that account for the above findings, we tested class-specific HDAC inhibitors including CI994 (HDAC class I), LMK235 (HDAC class II), 3-TYP (HDAC class III), and SAHA (HDAC pan inhibitor) using the stage II system described above. The class II HDACi, LMK235 produced findings similar to the pan-HDACi and increased the proportion of CD34+CD45+ HSPCs (Fig. 4A and B). Furthermore, when examining the effect of the class II HDACi on the 7-gene expression panel, HDAC class II inhibition led to a more narrow induction of only HOXA5, HOXA9, HOXA10, ERG, and LCOR at day 3, while pan-HDACi, SAHA, already induced most of the 7 genes (Fig. 4C). However, at day 6 of culture, mRNA of all members of the 7 genes signature (HOXA5, HOXA9, HOXA10, RUNX1, ERG, SPI1, and LCOR) were significantly induced (Fig. 4D). These data demonstrate that class II HDAC inhibition is specifically involved in the differentiation of ESCs into HSPCs.

Acetylated-H3 Is Bound to the Promoter Region of the 7 Genes in the Presence of SAHA

HDAC inhibitors promote the acetylation of histones by inhibiting the activity of HDAC enzyme, leading to a more relaxed chromatin structure associated with gene transcription.²⁷ While the above studies show changes in the 7 genes signature (HOXA5, HOXA9, HOXA10, RUNX1, ERG, SPI1, and LCOR) by qPCR, we sought to confirm them using Western blot. The protein expression of all 7 genes is shown in Fig. 5A. To further confirm that SAHA-induced acetylated-H3 bound to the promoter of the key 7-gene (HOXA5, HOXA9, HOXA10, RUNX1, ERG, SPI1, and LCOR), we used ChIP-qPCR, where H3 regions were immunoprecipitated and qPCR was performed for the promoter region of each gene. There was enhanced binding of acetylated histone-H3 to the promoter region of all 7 genes, except for HOXA10 (Fig. 5B). Thus, SAHA increases acetylated H3 at the promoter region of the above genes, thereby enhancing transcription of 6 of the 7 genes (HOXA5, HOXA9, RUNX1, ERG, SPI1, and LCOR) associated with an engraftable ESC-derived HSPCs.¹⁸

HDACi Enhanced HSPCs and Engraftment in Immune Deficient Mice

We assessed whether the SAHA-treated HE-derived HSPCs enabled engraftment in immune deficient NSG mice. After differentiating HSPCs using the stage II system, all suspension and adherent cells were collected and injected intrafemorally into NSG mice after sublethal irradiation (225 cGy). After 10-12 weeks, we observed a significantly higher percentage of hCD45+ cells in the BM of mice that received SAHA-treated hESC-derived CD34+ cells (Fig. 6A and B). hCD45 cells were not found in peripheral blood and the spleen (data not shown). To confirm the FACS data in the BM, we performed the qRT-PCR with human CD45 primers. SAHA-treated BM showed more than 100-fold higher hCD45 mRNA expression (Fig. 6C) compared with controls. Attempts to do serial transplantation were unsuccessful (not shown). These results suggested that HSPCs generated from ESCs and under the influence of SAHA enhanced BM engraftment in an immune deficient mice compared with controls.

SAHA Expanded HSPCs and In Vitro Differentiation of NK Cells

To test whether HDACi affects differentiation and function of ESC-derived mature blood cells, we used *in vitro* differentiation to make NK cells.^{6,28} Both DMSO controls and SAHA treated EBs were differentiated to human CD34+CD45+ HSPCs using the stage II system. After collecting and washing, the same number of CD34+CD45+ cells from each group were differentiated into the NK cell lineage on irradiated OP9-DL4 cells in the presence of IL-7, IL-15, FLT3L, and SCF for 3 weeks, as we have previously described.^{6,28} In both groups, NK cells (CD45+CD56+, Fig. 6D) were generated. The absolute number of differentiated NK cells was not significantly different between the 2 groups (Fig. 6E), suggesting that *in vitro* differentiation of HSPCs with SAHA did not hinder their ability to differentiate into NK cells. However, considering the ~2 to 5× expansion at the iPSC to CD34+CD45+ HSPCs differentiation step in the presence of SAHA (Fig. 1D), the number of total NK cells generated with the same number of starting iPSCs is significantly greater (Fig. 6F). The functionality of ESC-derived NK cells was also tested by assessing for

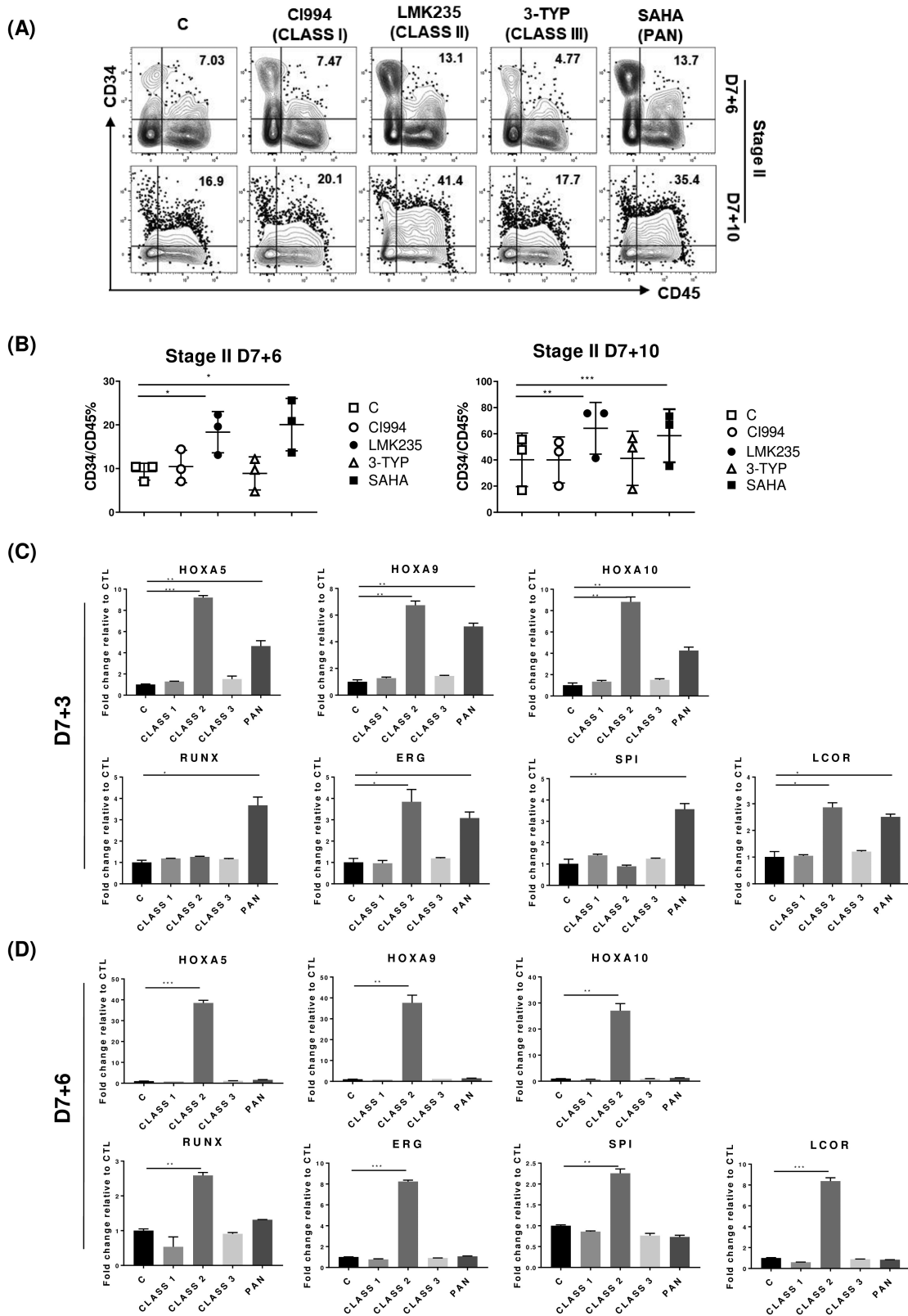


Figure 4. HDAC class II inhibitor enhanced the differentiation of HSPCs and the 7 genes overexpression. **(A)** Representative FACS plots of CD34+CD45+ hESCs were first made into spin EBs and differentiated with stage II method, then each HDAC inhibitor was added with the cytokine mixture at day 7 + 0; CI994 200 nM (HDAC class I), LMK235 100 nM (HDAC class II), 3-TYP 20 nM (HDAC class III), and SAHA 200 nM (HDAC pan inhibitor). Cells were harvested at day 7 + 6 and day 7 + 10. **(B)** Cumulative data showing CD34+CD45+ cells after treating HDAC inhibitor classes as in (A); $n = 3$, paired t -test, mean (SD), $*P < .05$; $**P < .01$; $***P < .001$. All cell fractions with the stage II method and the same concentration of HDAC inhibitors as (A) and (B) were harvested at day 7 + 3 (C) and day 7 + 6 (D), then had gene expression confirmed by qRT-PCR; $n = 3$, mean \pm SD, unpaired t -test, $*P < .05$; $**P < .01$; $***P < .001$, $****P < .0001$.

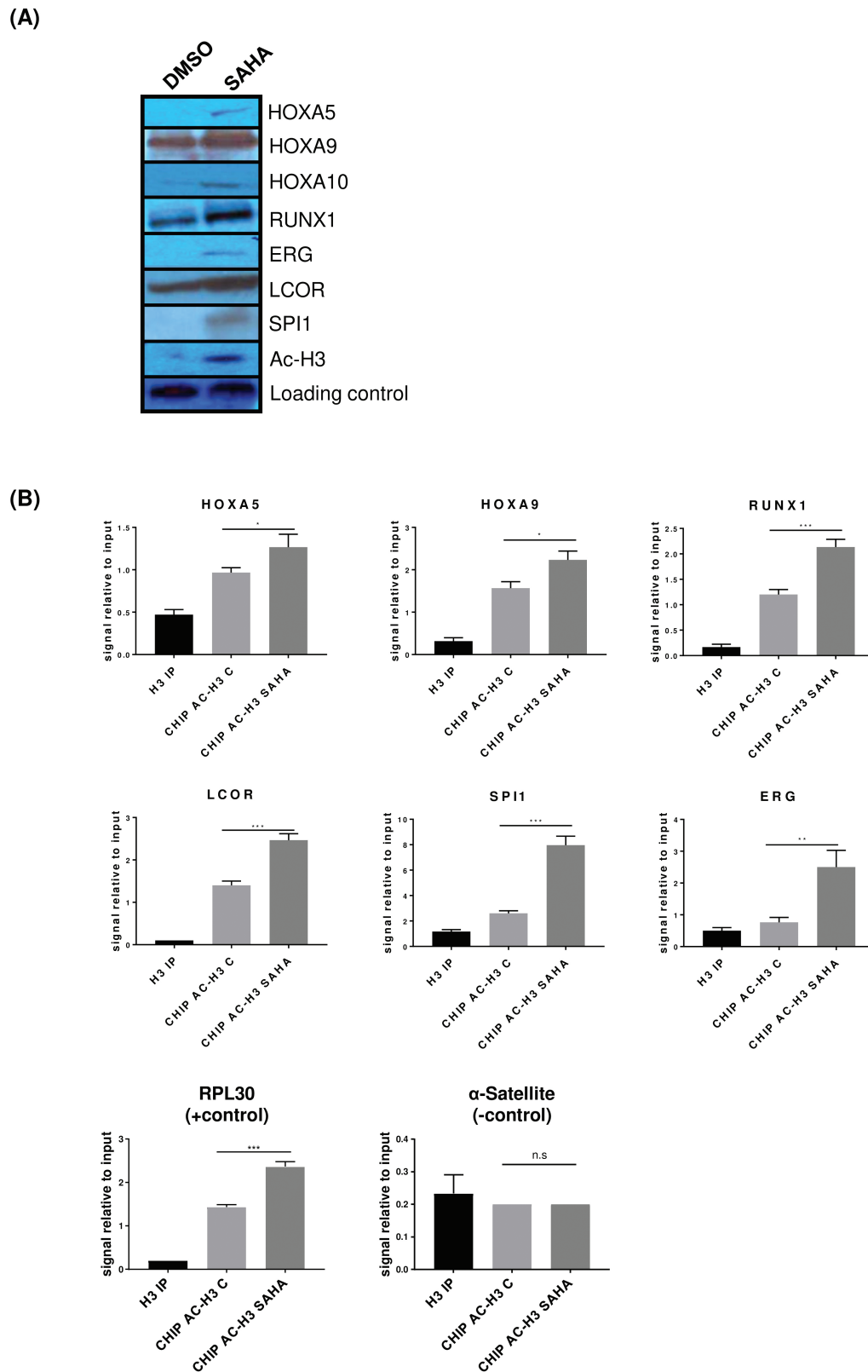


Figure 5. Acetylated-H3's binding at the promoter region of the 7 genes in the presence of SAHA. **(A)** At day 7 + 10, all cells differentiated with stage II method were harvested and protein-lysed for Western blot and lamin B1 was used as nuclear proteins' loading control. **(B)** CHIP qRT-PCR analysis was performed after differentiation with stage II system. H3 (histone 3) in a non-acetylated form was used as a control. RPL30 is a positive control for acetylated H3 and α -satellite is a negative control; $n = 3$, mean \pm SD, unpaired t -test, * $P < .05$; ** $P < .01$; *** $P < .001$.

degranulation after coculture with K562 cells. Both groups of NK cells showed transient expression of CD107a, consistent with degranulation (Fig. 6G). Moreover, we have performed

IncuCyte live cell imaging assays looking at the growth of malignant cells over time with and without NK cells that were differentiated from CD34+CD45+ HSPCs generated from

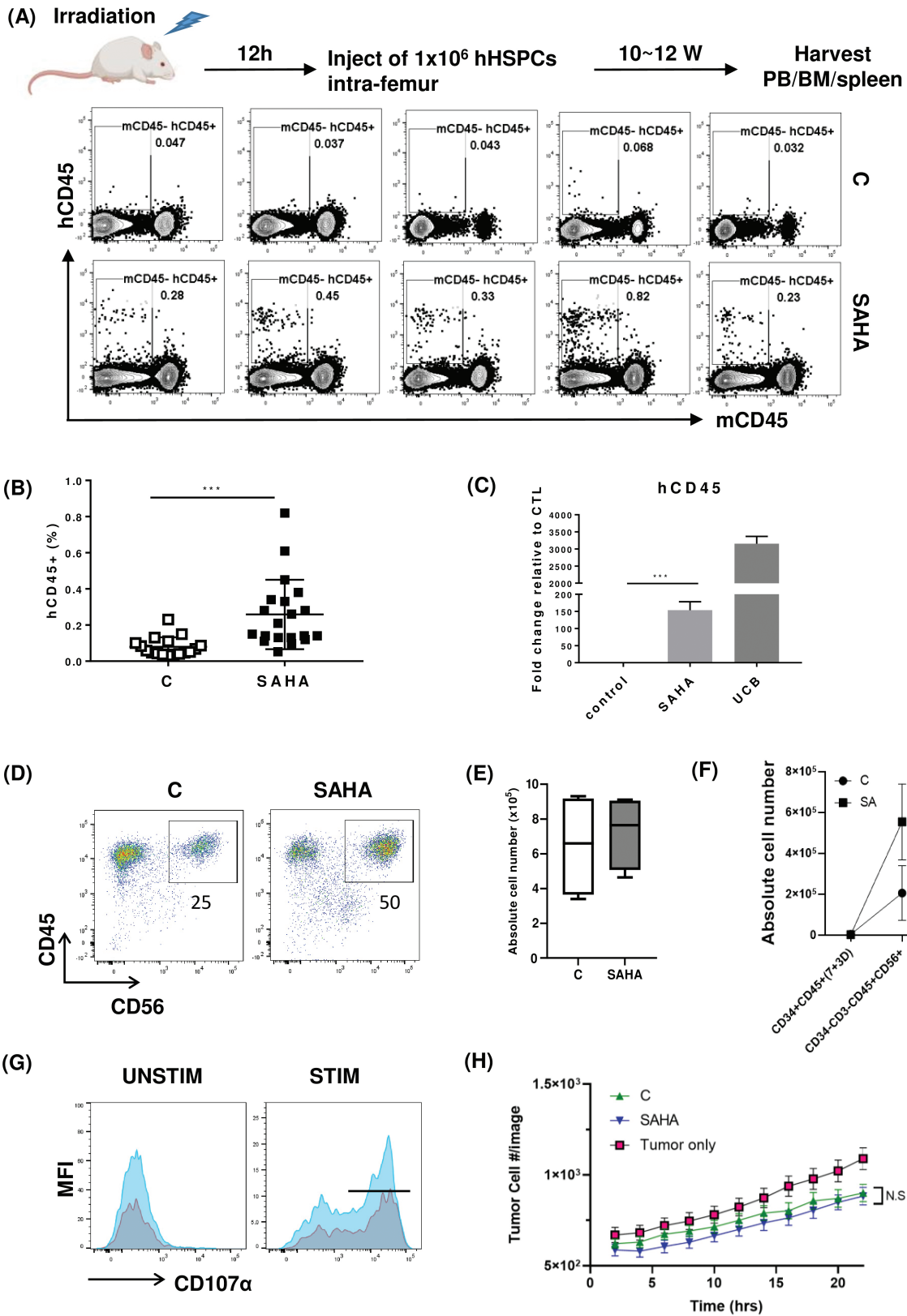


Figure 6. Effects of SAHA treatment in vivo and in vitro of hESC-derived HSPCs. **(A)** A design of the animal experiment. **(B)** Five representative FACS plots of human CD45+ and mouse CD45- cells in bone marrow from NSG mice. Data were collected from 3 separate experiments. **(B)** Quantification of total hCD45+mCD45- cells in bone marrow of NSG mice; $n = 20$, unpaired t -test, mean \pm SD. **(C)** Gene expression of human CD45 by qRT-PCR from the pooled bone marrow cells in each group. UCB was used as a positive control. Engrafted hCD45+mCD45- cells in UCB group were collected from mouse bone marrow after 12 weeks of cell injection; $n = 3$, error bars represent mean \pm SD using the paired t -test, $*** P < .001$. **(D)** Representative FACS plots after in vitro differentiation of hESCs-derived NK cells (CD45+CD56+). **(E)** The absolute cell number of CD45+CD56+ cells in control and SAHA group. $P =$ not significant. **(F)** The absolute cell number of CD34-CD3-CD45+CD56+ cells when the number of CD34+CD45+ cells were held constant. CD34+CD45+ cells were differentiated in SAHA or DMSO (control) and seeded the same number of cells in the NK cell differentiation

stage II cultures in the presence of SAHA or DMSO (control). As shown in Fig. 6H, both groups of NK cells decrease the malignant cell growth over time, consistent with cytotoxic response. However, there is no difference in the ability of HSPC-derived NKs to impair tumor growth between control NKs and SAHA-differentiated NKs. Collectively, these results show that compared with controls, SAHA increases the number of HPSCs in the early differentiation step and that these differentiate into mature lymphocytes (NK cells) at similar frequencies and with similar functionality, resulting in a higher total number of NK cells.

Discussion

Cell-based cancer immunotherapy using PSCs is moving to the clinic at a rapid pace. The appeal to this therapy is that is “off-the-shelf” and that PSCs can be genetically modified in ways that would be much more difficult with autologous cell products. While highly appealing, there are many challenges to the translation of PSCs to the clinic. A key barrier includes the relatively inefficient process of differentiation of pluripotent cells into the hematopoietic lineage (ie, the generation of HSPCs) and the lack of long-term HSC engraftment. To address the first issue, we tested the influence of HDAC inhibitors during the differentiation of hESC/iPSC cells to HSPCs, as a similar approach has been taken by others using UCB-derived CD34+ cells.⁷⁻⁹ We found that SAHA led to the expansion of hESC-derived HSPC progenitors and HSPCs by ~2- to 5-fold. While relatively meager, the cost of differentiating PSCs into HSPCs for downstream applications (ie, NK- or T-cell-based therapies) is material and thus, this simple maneuver is an important advance. As for the second barrier (ie, the generation of “engraftable HSCs”), we demonstrated that this approach gave rise to HSPCs that express a key genetic signature previously shown to be associated with HSPC engraftment in immune deficient mice (ie, HOXA5, HOXA9, HOXA10, RUNX1, ERG, SPI1, and LCOR).¹⁸ The expression of these 7 genes was also confirmed at the protein level and mechanistically, this occurred in a stage II-dependent manner, leading to the binding of acetylated histone 3 at the promoter region of these genes. However, this did not result in cells capable of serial engraftment in NSG mice.

Using 2 different methods of HSPC development, we show that HDAC inhibitors increased the production of HE that then go on to give rise to HSPCs. Interestingly, comparing the stages I and II differentiation systems, the stage I system was less impacted by SAHA than stage II. One of the key differences between these 2 systems is that the latter generates HE, leading us to focus on this as a potential intermediate to the HSPC differentiation under the influence of SAHA. By washing away the suspension cells in the stage II culture system (leaving only the adherent population, including HE) there were more HSPCs in the presence of SAHA. As well, using video microscopy we also observed budding of suspension cells from the adherent population which was likely the

HE (Supplementary Fig. S3). Mechanistically we examined the stage II cultures for the presence of a 7 gene signature, shown to mark engraftable HSPCs.¹⁸ These studies differ from prior work where researchers used lentiviral vectors to infect HE and overexpress the above-mentioned 7 genes, generating engraftable HSPCs.¹⁸

To further confirm that the increased expression of the 7 transcription factors was driven by HDAC inhibition, we assessed for the presence of acetylated histone H3 binding to the promoter region of these genes. Acetylated-H3 bound to the promoter region of 6 of the 7 genes, but not the promoter region in HOXA10, suggesting that other genes regulated by HDAC inhibitors drive HOXA10 expression. Future studies are needed to better understand the other proteins that cooperate with acetylated-H3 to increase the expression of these key 7 genes. In this regard, in our preliminary data, we used SAHA in RUNX1 overexpressed iPSCs and found further increases the expression of the 7 genes signature and higher numbers HSPCs and their progenitors (data not shown).

During differentiation of ESC to HSPCs, there is a critical window where the HSPCs emerge and then differentiate. In addition to increasing the production of HSPCs, SAHA-containing cultures had more stem cells at later time points, possibly suggesting that this agent prolongs the “stemness” of these cells by delaying differentiation. In support of this, RNA-seq showed the upregulation of specific genes involved in HSC lineage maintenance, including CD34, KIT, FLT3LG, and TPO. Additionally, the increased expression of these genes was present in both stages I and II systems treated with SAHA, perhaps explaining how SAHA functions to induce UCB CD34+ expansion. Regardless, stage II-derived HSPCs exposed to SAHA showed a higher increase of the above genes, suggesting cell stage intrinsic differences in the response to HDAC inhibition. Another interesting finding from the RNA-seq analysis was that stage I-derived HSPCs expressed genes known to appear later in the hematopoietic differentiation and in adaptive immune cells, such as CD3 and CD19 (Fig. 3B). Furthermore, HE-derived HSPCs cultured with SAHA showed an increase of many genes which are related to platelets such as CD9, GP5, GP9, and IL11. Interestingly, Zhu et al tested HDAC inhibitors in CD34+ cells from human BM or UCB and found the overexpression of MkP differentiation related genes including MZF1, GSX2, HOXC6, HDAC11, HES7, FOXB1, MXD3, HOXA9, NFATC1, NPAS1, FLI1, and PCGF2.²⁹ We too found that most of these genes overexpressed in our cultures. Based on Zhu et al²⁹ and our study, HDAC inhibitors potentially regulate platelet production through the expression of genes that drive megakaryopoiesis.

Additionally, cell adhesion and chemokine signaling KEGG pathways were enriched with several genes that are advantageous for engraftment. For example, both CXCR5 (known to be involved in T- and B-cell homing)^{24,25} and CX3CR1 (reported to control T-cell homing)²⁶ were increased in HE-derived HSPCs in the presence of HDAC inhibitors. As

conditions. After 3 weeks NK differentiation, the number of cells were counted; $n = 10$, error bars represent mean \pm SD using the paired t -test, **** $P < .0001$. (G) CD107a expression from NK cells. CD45+CD56+ cells were collected and stimulated with K562 cells. Left plot represents unstimulated condition and right plot is K562 stimulated condition. Red; control, blue; SAHA. (H) NK-tumor coculture effect on tumor growth. Cells were differentiated for 4 weeks with stage II differentiated CD34+CD45+ cells. Differentiated NK cells were stimulated with 10 ng/mL IL-12 and 10 ng/mL IL-18 for overnight. NK cells were then cocultured with the pre-plated (mCherry) expressing RH30 cells at 1:1 ratio (tumor: NK) in 96-well plate using NK media. The plates were scanned every 2 hours for 24 hours by using IncuCyte. Tumor growth was measured by detecting mCherry expression. Error bars represent standard error of the mean (SD), 2-way ANOVA. $P =$ not significant.

well, various integrin and ICAM genes are overexpressed in HE-derived HSPCs treated with SAHA (supplementary Fig. 6). Given these findings and the expression of the 7 gene pattern previously shown to drive engraftable pluripotent cell-derived HSPCs, we tested whether SAHA-treated cells could engraft in immune deficient mice. While we observed a higher proportion of cells engrafting in the SAHA-treated group, serial transplantation experiments were unsuccessful, suggesting that despite acquiring a 7-gene signature associated with engraftable PSC-derived HSPCs, SAHA treated CD34+CD45+ cells had not acquired this property. The reasons for this are not clear, but we speculate that while SAHA may positively influence a key genetic signature previously shown to be associated with HSPC engraftment in immune deficient mice (ie, HOXA5, HOXA9, HOXA10, RUNX1, ERG, SPI1, and LCOR)¹⁸ it may also negatively affect other genes important in engraftment.

Notwithstanding, there is considerable effort in creating ESC/iPSC-derived cell products in vitro, including red blood cells, platelets, and effector lymphocytes for cancer therapy. We and others have described methods to create NK cells from ESC/iPSCs and these are now being translated clinically with encouraging safety and efficacy in early phase I data.³⁰ As above, one key bottleneck in the differentiation process is that from pluripotency to the commitment to the hematopoietic lineage. We found that SAHA could influence HSPCs development and that it did not interfere with the differentiation and/or functionality of NK cells after removing SAHA (only present during the development of CD34+CD45+ cells). Given the real bottleneck of differentiating PSCs into HSPCs and the ease of adoption, the use of SAHA in protocols to create iPSC-derived cell products seems like a reasonable and cost-effective approach.

Conclusion

Altogether, through this work we demonstrate that the addition of SAHA during the differentiation of PSCs into HSPCs led to higher numbers of CD34+ HSPCs that show an induction of the 7 genes signature previously associated with an engraftable HSPC. Mechanistically, this observation occurs via HE-derived HSPCs and the inhibition of HDAC II accounts for these findings. We show that while there was enhanced primary engraftment in mice, serial transplantation was not possible in our system. These effects might be due to either HDAC inhibitor associated de-repression of other genes or because the effects of the drug are only transient. We show that HSPCs derived from this SAHA system can be differentiated into functional NK cells. Given that HSPC expansion from SAHA was 2 to 5 times greater than controls, use of SAHA may overcome a significant barrier in the application of PSCs-derived lymphocytes for clinical applications.

Acknowledgments

This work was supported in part by following Gates Center Grubstake Grant and NIH (NIH 1R01AI100879). The project described was supported in part by award number 5P30CA046934-30 from the National Cancer Institute. The content is solely the responsibility of the authors and does not necessarily represent the official views of the National Cancer Institute or the National Institutes of Health.

Funding

This work was supported in part by following Gates Center Grubstake Grant and NIH (NIH 1R01AI100879). The project described was supported in part by award number 5P30CA046934-30 from the National Cancer Institute.

Conflict of Interest

M.V. and S.-H.S. declared a patent protection application on some of the material contained in this manuscript. The other authors declare no potential conflicts of interest.

Author Contributions

S.-H.S.: conception and design, collection and assembly of data, data analysis and interpretation, writing manuscript; R.W.: collection and assembly of data; T.D.G. and K.J.: analyzed sequencing data; T.S., A.Y., J.L., D.T., L.C., and D.J.: provided technical assistance; M.R.V.: data interpretation, writing, and final approval of manuscript.

Data Availability

The data underlying this article will be shared on reasonable request to the corresponding author.

Supplementary Material

Supplementary material is available at *Stem Cells Translational Medicine* online.

References

1. Locke FL, Ghobadi A, Jacobson CA, et al. Long-term safety and activity of axicabtagene ciloleucel in refractory large B-cell lymphoma (ZUMA-1): a single-arm, multicentre, phase 1-2 trial. *Lancet Oncol.* 2019;20(1):31-42.
2. Maude SL, Laetsch TW, Buechner J, et al. Tisagenlecleucel in children and young adults with B-cell lymphoblastic leukemia. *N Engl J Med.* 2018;378(5):439-448.
3. Liu E, Marin D, Banerjee P, et al. Use of CAR-transduced natural killer cells in CD19-positive lymphoid tumors. *N Engl J Med.* 2020;382(6):545-553.
4. Miller JS, Soignier Y, Panoskaltsis-Mortari A, et al. Successful adoptive transfer and in vivo expansion of human haploidentical NK cells in patients with cancer. *Blood.* 2005;105(8):3051-3057.
5. Ueda T, Kaneko S. In vitro differentiation of T cell: from CAR-modified T-iPSC. *Methods Mol Biol.* 2019;2048:85-91.
6. Angelos MG, Ruh PN, Webber BR, et al. Aryl hydrocarbon receptor inhibition promotes hematolymphoid development from human pluripotent stem cells. *Blood.* 2017;129(26):3428-3439.
7. Huang X, Guo B, Liu S, Wan J, Broxmeyer HE. Neutralizing negative epigenetic regulation by HDAC5 enhances human haematopoietic stem cell homing and engraftment. *Nat Commun.* 2018;9(1):2741.
8. Chaurasia P, Gajzer DC, Schaniel C, D'Souza S, Hoffman R. Epigenetic reprogramming induces the expansion of cord blood stem cells. *J Clin Invest.* 2014;124(6):2378-2395.
9. Arulmozhivarman G, Krater M, Wobus M, et al. Zebrafish in-vivo screening for compounds amplifying hematopoietic stem and progenitor cells: - preclinical validation in human CD34+ stem and progenitor cells. *Sci Rep.* 2017;7(1):12084.
10. Young JC, Wu S, Hanstean G, et al. Inhibitors of histone deacetylases promote hematopoietic stem cell self-renewal. *Cytotherapy.* 2004;6(4):328-336.
11. Peled T, Shoham H, Aschengrau D, et al. Nicotinamide, a SIRT1 inhibitor, inhibits differentiation and facilitates expansion of

- hematopoietic progenitor cells with enhanced bone marrow homing and engraftment. *Exp Hematol.* 2012;40(4):342-355 e341.
12. Horwitz ME, Wease S, Blackwell B, et al. Phase I/II study of stem-cell transplantation using a single cord blood unit expanded ex vivo with nicotinamide. *J Clin Oncol.* 2019;37(5):367-374.
 13. Horwitz ME, Stiff PJ, Cutler CS, et al. Omidubicel versus standard myeloablative umbilical cord blood transplantation: results of a phase III randomized study. *Blood.* 2021;138(16):1429-1440.
 14. Slukvin, II. Generating human hematopoietic stem cells in vitro -exploring endothelial to hematopoietic transition as a portal for stemness acquisition. *FEBS Lett.* 2016;590(22):4126-4143.
 15. Choi KD, Vodyanik MA, Togarrati PP, et al. Identification of the hemogenic endothelial progenitor and its direct precursor in human pluripotent stem cell differentiation cultures. *Cell Rep.* 2012;2(3):553-567.
 16. Kennedy M, D'Souza SL, Lynch-Kattman M, Schwantz S, Keller G. Development of the hemangioblast defines the onset of hematopoiesis in human ES cell differentiation cultures. *Blood.* 2007;109(7):2679-2687.
 17. Guibentif C, Ronn RE, Boiers C, et al. Single-cell analysis identifies distinct stages of human endothelial-to-hematopoietic transition. *Cell Rep.* 2017;19(1):10-19.
 18. Sugimura R, Jha DK, Han A, et al. Haematopoietic stem and progenitor cells from human pluripotent stem cells. *Nature.* 2017;545(7655):432-438.
 19. Grzywacz B, Kataria N, Kataria N, Blazar BR, Miller JS, Verneris MR. Natural killer-cell differentiation by myeloid progenitors. *Blood.* 2011;117(13):3548-3558.
 20. Nishikawa SI, Nishikawa S, Kawamoto H, et al. In vitro generation of lymphohematopoietic cells from endothelial cells purified from murine embryos. *Immunity.* 1998;8(6):761-769.
 21. Bhatlekar S, Fields JZ, Boman BM. Role of HOX genes in stem cell differentiation and cancer. *Stem Cells Int.* 2018;2018:3569493.
 22. Fan R, Bonde S, Gao P, et al. Dynamic HoxB4-regulatory network during embryonic stem cell differentiation to hematopoietic cells. *Blood.* 2012;119(19):e139-147.
 23. Dou DR, Calvanese V, Sierra MI, et al. Medial HOXA genes demarcate haematopoietic stem cell fate during human development. *Nat Cell Biol.* 2016;18(6):595-606.
 24. Schaerli P, Willimann K, Lang AB, Lipp M, Loetscher P, Moser B. CXCR5 chemokine receptor 5 expression defines follicular homing T cells with B cell helper function. *J Exp Med.* 2000;192(11):1553-1562.
 25. Hopken UE, Achtman AH, Kruger K, Lipp M. Distinct and overlapping roles of CXCR5 and CCR7 in B-1 cell homing and early immunity against bacterial pathogens. *J Leukoc Biol.* 2004;76(3):709-718.
 26. Combadiere B, Faure S, Autran B, Debre P, Combadiere C. The chemokine receptor CX3CR1 controls homing and anti-viral potencies of CD8 effector-memory T lymphocytes in HIV-infected patients. *AIDS.* 2003;17(9):1279-1290.
 27. Bose P, Dai Y, Grant S. Histone deacetylase inhibitor (HDACI) mechanisms of action: emerging insights. *Pharmacol Ther.* 2014;143(3):323-336.
 28. Woll PS, Grzywacz B, Tian X, et al. Human embryonic stem cells differentiate into a homogeneous population of natural killer cells with potent in vivo antitumor activity. *Blood.* 2009;113(24):6094-6101.
 29. Zhu F, Feng M, Sinha R, Seita J, Mori Y, Weissman IL. Screening for genes that regulate the differentiation of human megakaryocytic lineage cells. *Proc Natl Acad Sci USA.* 2018;115(40):E9308-E9316.
 30. Paolo S, Veronika B, Aaron G et al. Preliminary results of a phase I trial of FT516, an off-the-shelf natural killer (NK) cell therapy derived from a clonal master induced pluripotent stem cell (iPSC) line expressing high-affinity, non-cleavable CD16 (hnCD16), in patients (pts) with relapsed/refractory (R/R) B-cell lymphoma (BCL). *Journal of Clinical Oncology.* 2021;39(15_suppl):7541-7541